ELECTROMAGNETIC-THERMAL ANALYSIS OF AN RF RECTANGULAR RESONANT CAVITY APPLICATOR FOR HYPERTHERMIA TARGETING DEEP-SEATED TUMORS USING A HUMAN BODY MODEL WITH BLOOD FLOW AND FAT LAYER

Yutaka TANGE[1], Yasushi KANAI[2] and Yoshiaki SAITOH[3]

Maxwell's and heat transfer equations were coupled and solved to determine the heating characteristics of an RF rectangular resonant cavity applicator for hyperthermia before the clinical stage. A simple human body model with blood flow and a fat layer was constructed. The region unaffected by tumor was shielded from electromagnetic fields by using conductive caps. The surface of the human model that was exposed to the electromagnetic fields was cooled with pure water bolus. Calculated results show that this applicator can heat a deep-seated tumor.

Key words: deep-seated tumors, hyperthermia, resonant cavity applicators, blood flow, human organ.

1. Introduction

Cancer is the uncontrolled growth and spread of cells. It can affect almost any part of the body. The growths often invade the surrounding tissues and even metastasize to distant sites [1]. Therefore, it is desirable to remove the cancer from the human body as soon as possible.

Hyperthermia is a cancer therapy that focuses on the differences in the heating sensitivity of a tumor. In comparison to a non-tumor cells that live up to 44°C, the tumor dies above 42.5°C. By using electromagnetic energy, the tumor cells are heated up to a temperature at which they die.

Heating devices for noninvasive hyperthermia, for example radiofrequency and microwave heating applicators [2], have already been developed. However, deep-seated tumors cannot be sufficiently heated by these devices because of the complex human tissues and the cooling effect caused by the blood flow. A phased array system [3] with multiple antennas can focus the electromagnetic energy on a deep-seated tumor. However, it is very difficult to determine the optimum amplitude and phase of power for each patient. In recent experimental studies, very small implants [4] and magnetic fluids have been developed; they can heat a tumor using an inductive heating applicator. The question is how to focus the energy on local regions containing the tumor in the human body. Numerical studies have reported a new heating technique—the annular-shaped inductive aperture-type applicator [5] has been reported. In the report, a cylindrical body with a fat layer was used. Although heat generation was possible in deep regions of the body, it was noted that the heating occurred between the muscle and the fat layer.

We have already reported a reentrant cavity applicator that targets deep-seated tumors [6, 7]; the deep region of a small disk-shaped dielectric phantom could be heated. We also have developed an RF rectangular resonant cavity applicator for a larger model with deep-seated tumors. By optimizing the positions of multiple antennas in the applicator, we heated the deep interior of the phantom [8–10]. In order to realize local heating, conductive caps were attached to the dielectric phantom. As a result, we could heat the selective region. Before the clinical stage, it is necessary for us to model the components of a human body accurately, e.g., blood flow, human organs, and the fat layer.

In this paper, we investigate the heating characteristics of an RF rectangular resonant cavity applicator for deep-seated tumors before the clinical stage. Simulation results show that this applicator can heat deep-seated tumors. Therefore, it is possible to apply this RF cavity applicator in the clinical stage for

1 Assistant Professor, Dept. of Electrical and Computer Eng., Maizuru National College of Technology.
2 Professor, Dept. of Information and Electronics Eng., Niigata Institute of Technlogy.
3 Professor Emeritus, Niigata University.

heating deep-seated tumors.

2. RF rectangular resonant cavity applicator

The experimental setup used in our study is illustrated in Fig. 1 [9, 10]. The applicator consists of a copper plate with the following dimensions: 1300 mm length × 1500 mm width × 1450 mm height × 0.5 mm thickness.

In the cavity applicator, conductive caps were attached to the object to be heated and the object was placed on a wooden table. Note that the caps protect the normal cells from the electromagnetic field. In addition, the caps enable efficient heating of the local region. An L-type antenna was fabricated from a copper pipe. As shown in Fig. 2, the antenna is placed at the optimum point x = –450 mm for heating the deep region.

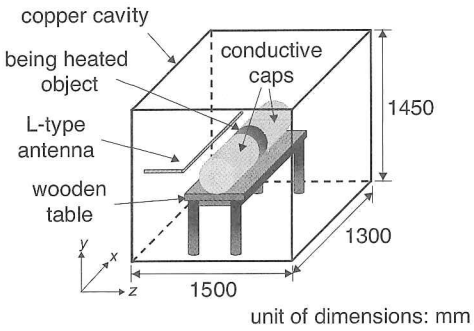

Fig. 1 Experimental setup used in our study.

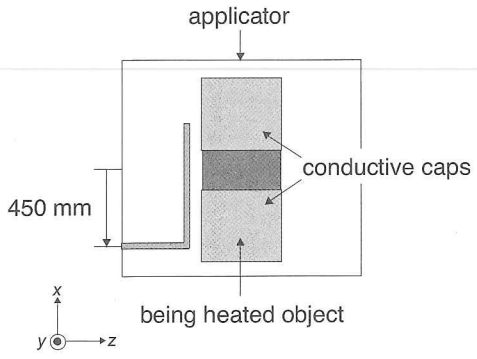

Fig. 2 Setup of the antenna and the object to be heated. Optimum feeding point of the L-type antenna was x = –450 mm.

3. Electromagnetic-heat transfer equation considering the blood flow

For analyzing the electromagnetic field in the cavity, we solved Maxwell's equations using the three-dimensional finite-difference time-domain (FDTD) method [11].

$$\nabla \times \mathbf{E} = -\mu \frac{\partial \mathbf{H}}{\partial t}, \quad \nabla \times \mathbf{H} = \sigma \mathbf{E} + \varepsilon \frac{\partial \mathbf{E}}{\partial t} \tag{1}$$

where μ, σ, and ε represent the permeability, electrical conductivity, and permittivity, respectively. The wire approximation method [12] was used to model the L-type antenna. A voltage source supplied a sinusoidal output. In the electromagnetic analysis, we first derived the resonant frequencies in the cavity. Then, the electromagnetic energy at the lowest resonant frequency was applied. After analyzing the fields, the object that was heated by using the electromagnetic energy was examined using the following formula.

$$W_h = \frac{1}{T}\sigma \int |\mathbf{E}|^2 dt \tag{2}$$

The time-dependent heat-transfer equations [13]

$$\rho c \frac{\partial T}{\partial t} = \lambda \nabla^2 T + Q \tag{3}$$

$$Q = -W_c + W_h \tag{4}$$

$$q = \alpha_c (T - T_c) \tag{5}$$

are solved by the three-dimensional finite-element method (FEM); in the above equations, ρ, c, λ, Q, q, α_c, and T_c denote the volume density of the organ, specific heat capacity of the organ, thermal conductivity of the organ, heat generation by considering the cooling effect of the blood flow W_c and the electromagnetic energy W_h, heat flux, heat transfer coefficient, and external temperature, respectively. The cooling energy is defined by the following equation:

$$W_c = (F\rho)(\rho_b c_b)(T - T_b) \tag{6}$$

In this equation, F, ρ_b, c_b, and T_b denote the amount of blood flow per unit time in the organ, volume density of blood, specific heat capacity of blood, and temperature of blood, respectively; T_b is constant at 37°C. F is given by the following expression:

$$F = F_s \exp(0.0957 B_r (T - T_b)) \tag{7}$$

The value of F depends on the tissue temperature, where F_s is the amount of blood flowing in the organ at 37°C and B_r is the temperature dependence of the metabolic rate. In the heat transfer analysis, the step-by-step reevaluation of the temperatures in equations (6) and (7) is performed considering this cooling effect.

4. Cavity applicator and simple human body model used for calculation

In the electromagnetic analysis, we modeled an L-type antenna, a simple human body model with blood flow and fat layer, and a rectangular resonant cavity applicator. As shown in Fig. 3, we have modeled the human organs with blood flow, such as muscles, fat, liver, stomach, kidneys, lungs, and the deep-seated tumor in the liver. As shown in Fig. 4, we divided the applicator containing the human model into regular 25mm finite-difference cells [13]. The electromagnetic energy was interpolated every 12.5 mm because we used an FEM brick element with a side length of 12.5 mm in the thermal analysis. The electric and thermal properties are given in Table 1 [14]. The wooden table used in the experiments was not considered in the calculations because it did not have a major influence on the electromagnetic-thermal analysis.

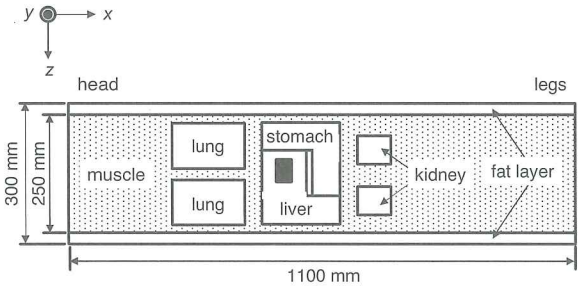

(a) Central z–x plane of the human model.

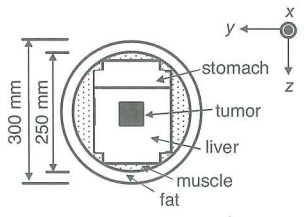

(b) Central y-z plane of the human model.

Fig. 3 Human body model with a fat layer.

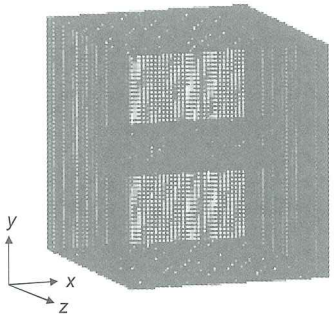

Fig. 4 Finite-difference cell models of an RF rectangular resonant cavity applicator used for the electromagnetic analysis. An L-type antenna, a simple human body model with fat layer, and conductive caps are modeled.

Table 1 Electric and thermal properties of the main organs of the human body.

	ε_r	σ [S/m]	λ [W/m°C]	ρ [kg/m^3]	c [J/kg°C]	F_s [m^3/kg s]	B_r [1/°C]
fat	8.5	0.06	0.220	900	2300	5.00×10^{-7}	0.6
muscle	72	0.80	0.600	1020	3500	83.0×10^{-7}	1.0
tumor	78	0.89	0.570	1040	3900	5.00×10^{-7}	0.0
liver	78	0.60	0.560	1020	3500	144×10^{-7}	0.8
stomach	77	0.51	0.560	1020	3500	50.0×10^{-7}	0.6
kidney	89	1.0	0.560	1020	3500	667×10^{-7}	0.8
lungs	40	0.35	0.480	300	3500	722×10^{-7}	0.8

5. Results and discussion

The calculated results are shown in Figs. 5–9; where the antenna is placed as shown in Fig. 2. The starting temperature T_0, room temperature T_c, and resonance frequency f_r for each condition are listed in the figure captions.

(a) Case in which the fat layer is ignored

Fig. 5 shows the electromagnetic energy and temperature distributions of the simple human model without the fat layer. In Fig. 5 (a), it is found that the energy is concentrated in the surface region. In addition, it is observed that the energy is slightly focused on regions with low conductivity, for example, the stomach and liver regions that are affected by the tumor. As shown in Fig. 5 (b), the tumor is heated because of little blood flow through it. The temperature increase in the other body parts is limited because of the increase in the blood flow with the temperature. Fig. 6 shows the temperature increase in the surface region and the

deep-seated liver tumor. It is found that only the tumor region has a high temperature. Therefore, it may be stated that this applicator can heat the deep-seated liver tumor in case there is no fat layer.

(b) Case in which the fat layer is considered

Fig. 7 shows the electromagnetic energy and temperature distributions in the case of the simple human model with a fat layer. In Fig. 7 (a), it is observed that the electromagnetic energy is focused on the boundary between the muscle and the fat layer. Moreover, this energy is mainly focused on the liver and the stomach. As observed in Fig. 7 (b), the deep-seated liver tumor is heated to a high temperature. However, it is necessary to reduce the surface temperature by using a cooling system such as a water bolus. Fig. 8 shows the temperature distribution of the model when a pure water bolus is employed. It can be observed that the surface region was cooled. The increase in temperatures of the tumor and the surface region with and without the bolus is shown in Fig. 9; It is observed that the water bolus cools only the surface region significantly, and it does not cool the tumor. Therefore, it may be possible to use this cavity applicator with the water bolus for heating deep-seated tumors.

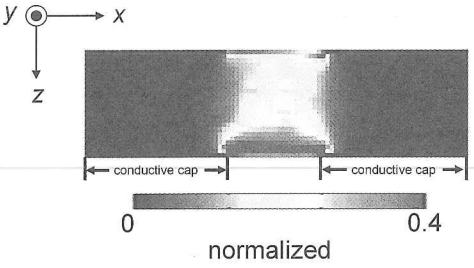

(a) Electromagnetic energy distribution.

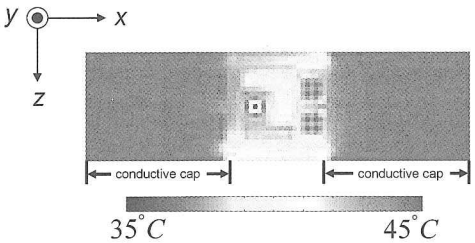

(b) Temperature distribution.

Fig. 5 Electromagnetic energy and temperature distributions for the simple human model without a fat layer. Here, T_0, T_c, and f_r are 37°C, 24°C, and 63.17 MHz, respectively.

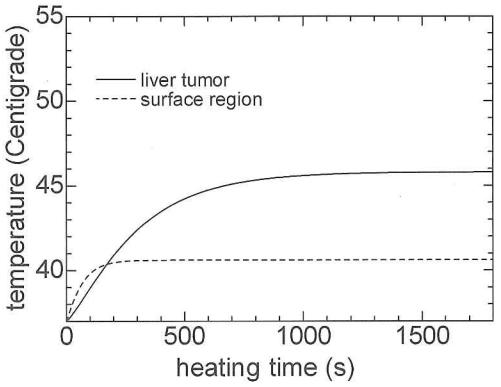

Fig. 6 Temperature increases in the surface region and deep-seated tumor.

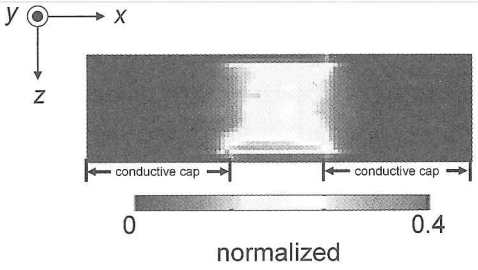

(a) Electromagnetic energy distribution.

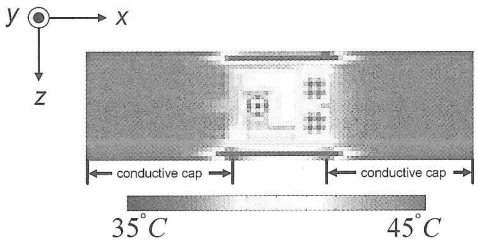

(b) Temperature distribution.

Fig. 7 Electromagnetic energy and temperature distribution for the simple human model with a fat layer. Here, T_0, T_c, and f_r are 37°C, 24°C, and 63.07 MHz, respectively.

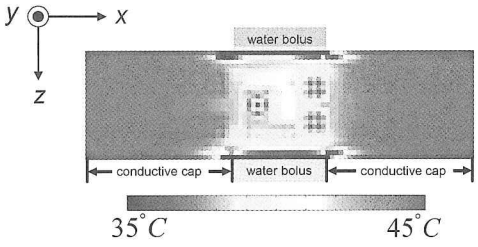

Fig. 8 Temperature distribution on fat layer and tumor under the application of a pure water bolus. Results are shown in the central zx-plane.

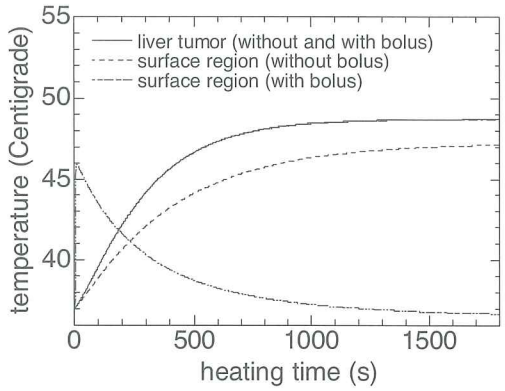

Fig. 9 Temperature increase in the surface region and deep-seated tumor with and without the water bolus.

6. Conclusion

The heating characteristics for an RF hyperthermic system by using a rectangular resonant cavity applicator have been investigated numerically for application to deep-seated tumors. Before the clinical stage, a simple human body model with blood flow and a fat layer was modeled and analyzed. We obtained improved heating patterns for a deep-seated tumor as compared to those obtained in our previous studies. Therefore, this applicator is suitable for the heating of deep-seated tumors in hyperthermic treatment.

7. References

[1] World Health Organization web site [Online]. Available: http://www.who.int/cancer/en/.

[2] K. Ito and K. Saito, "Microwave antennas for thermal therapy," *Japanese Society for Thermal Medicine*, vol. 23, no. 1, pp. 23–30, Mar. 2007.

[3] N. Siauve, L. Nicolas, C. Vollaire, A. Nicolas, and J. A. Vasconcelos, "Optimization of 3-D SAR distribution in local RF hyperthermia," *IEEE Trans. on Magn.*, vol. 40, no. 2, pp. 1264–1267, Mar. 2004.

[4] Y. Kotsuka and H. Okada, "Development of small and high efficiency implant for deep local hyperthermia," *Jpn. J. Hyperthermic Oncol.*, vol. 19, no.1, pp. 11–22, Mar. 2003.

[5] H. Kato, M. Kuroda, K. Shibuya, and A. Kanazawa, "Focused deep heating with an inductive type applicator," *Thermal Medicine*, vol. 23, no. 3, pp.133–143, Oct. 2007.

[6] K. Kato, J. Matsuda, and Y. Saitoh, "A re-entrant type resonant cavity applicator for deep-seated hyperthermia treatment," *Proc. Annual Int'l Conf. of the IEEE Eng. in Medicine and Biology Society*, vol. 11, pp. 1712–1713, Nov. 1989.

[7] Y. Kanai, T. Tsukamoto, K. Toyama, Y. Saitoh, M. Miyakawa, and T. Kashiwa, " Analysis of a hyperthermic treatment in a reentrant resonant cavity applicator by solving time-dependent electromagnetic-heat transfer equations," *IEEE Trans. on Magn.*, vol. 32, no. 3, pp. 1661–1664, May 1996.

[8] S. Soeta, S. Yokoo, M. Shimada, Y. Kanai, and J. Hori, "Eigenmode analysis of a parallelepiped resonator for hyperthermic treatment by using FD-TD method," *10th Niigata Branch Regional Meeting of IEE Japan*, III-21, Nov. 2001 (in Japanese).

[9] Y. Tange, Y. Kanai, and Y. Saitoh, "Analysis and development of a radio frequency rectangular resonant cavity applicator with multiple antennas for a hyperthermic treatment," *IEEE Trans. on Magn.*, vol. 41, no. 5, pp. 1880–1883, May 2005.

[10] Y. Tange, Y. Kanai, Y. Saitoh, and T. Kashiwa, "New heating characteristics of a radio frequency rectangular resonant cavity applicator using various antennas for hyperthermic treatment," *ACES Journal*, vol. 22, no. 2, pp. 269–276, July 2007.

[11] D. Sullivan, "Three-dimensional computer simulation in deep regional hyperthermia using the finite-difference time-domain method," *IEEE Trans. on Microwave Theory Tech.*, vol. 38, no. 2, pp. 204–211, Feb. 1990.

[12] K. R. Umashankar, A. Taflove, and B. Beker, "Calculation and experimental validation of induced currents on coupled wires in an arbitrary shaped cavity," *IEEE Trans. on Antennas Propagat.*, vol. 35, no. 11, pp. 1248–1257, Nov. 1987.

[13] Y. Kanai and K. Sato, "Automatic mesh generation for 3D electromagnetic field analysis by FD-TD method," *IEEE Trans. on Magn.*, vol. 34, no. 5, pp. 3383–3386, Sep. 1998.

[14] Y. Kanai, T. Tsukamoto, Y. Saitoh, M. Miyakawa, and T. Kashiwa, "Analysis of a hyperthermic treatment using a reentrant resonant cavity applicator for a heterogeneous model with blood flow," *IEEE Trans. on Magn.*, vol. 33, no. 2, pp. 2175–2178, Mar. 1997.

(Received November 6, 2009)